Performance and Emission Characteristics of Dual Fuel Engines at Part Loads Using Simultaneous Effect of Exhaust Gas Recirculation and Pre-Heating of In-let Air

A. Paykani[1], R. Khoshbakhti Saray[2] , A. M. Kousha[1], and M. T. Shervani Tabar[1]

[1] Department of Mechanical Engineering, University of Tabriz, Tabriz, Iran

[2] Department of Mechanical Engineering, Sahand University of Technology, New Town of Sahand, Iran

* ...@iust.ac.ir

Abstract

In this study, a numerical simulation using the CFD software, FLUENT, has been conducted to examine the effect of various shapes of the venturi component sections in order to find the optimum venturi specifications to increase the EGR rate with minimum pressure loss at the part load operation range. The CFD results reveal that the venturi should be precisely optimized to introduce the required amount of EGR to the engine manifold. Then, the optimum venturi was manufactured, and it was installed on the engine intake system. By using the optimum Venturi EGR system instead of original system the 26% increase in EGR flow rate to the engine manifold is observed. In the second part of the paper, an experimental investigation was carried out on a "Lister 8-1" dual fuel (diesel – natural gas) engine to examine the simultaneous effect of inlet air pre-heating and EGR on performance and emission characteristics of a dual fuel engine. The use of EGR at high levels seems to be unable to improve the engine performance at part loads, however, it is shown that EGR combined with pre-heating of inlet air can slightly increase thermal efficiency, resulting in reduced levels of both UHC and NOx emissions. CO and HC emissions were reduced by 24% and 31%, respectively. The NO_x emissions were decreased by 21% because of the lower combustion temperature due to the much inert gas brought by EGR and decreased oxygen concentration in the cylinder.

1. INTRODUCTION

The use of alternative gaseous fuels in diesel engines continues to be strong due to environmental concerns and their relatively increased availability at low prices. Natural gas satisfies previous requirements. It has a high octane number and therefore it is suitable for engines with relatively high compression ratio [1-2]. Moreover When burnt, it produces insignificant SOx and relatively little NO_x, the main constituents of acid rain, and substantially less CO_2, a key element in the greenhouse debate, than most oil products and coal [3].

The operation of diesel engines on gaseous fuels, commonly known as dual fuel engines, uses diesel fuel as the pilot fuel and gaseous fuel (natural gas in the present work) as the main fuel. Dual fuel engines are one of the possible short-term solutions to reduce emissions from traditional diesel engines, meanwhile, utilizing an alternative fuel like natural gas as primary fuel. It consequently results not only in an interesting technology to meet future emissions regulations, but also a powerful solution to retrofit existing engines [4]. In this method, natural gas is premixed with fresh air in the intake manifold, which then undergoes a multi-point ignition due to the compression-ignition and combustion of a pilot diesel fuel spray. Then, flame propagates through the premixed natural gas mixture. Thus, dual fuel operation with natural gas fuel can yield a high thermal efficiency almost comparable to the same engine operating on diesel fuel at higher loads. However, engine performance and emissions suffer at low loads when operating in dual fuel mode [5-6]. During part load engine operation, the fuel gas supply is reduced by means of a gas control valve. However, a simultaneous reduction of the air supply decreases the air quantity induced. Hence, the compression pressure and the mean effective pressure of the engine are decreased. This would finally lead to a drop in power and efficiency. One reason for this is resulting from overall very lean mixtures at low loads. The lean mixtures ignite very hard and burn slowly [7]. Exhaust gas recirculation (EGR) is one of the most effective methods for reducing the emissions of NO_x of diesel engines. EGR system has already been used to mass -

produced diesel engines, in which EGR is used at the low and medium load of engine operating condition, resulting in effective NOx reduction [8]. The EGR in dual fuel engine may be used for improving part load operation and reducing the exhaust emissions of NOx. Introduction of hot EGR has combinations of some these effects [9]:

1) Depletion of oxygen in the intake charge
2) Increased intake temperature due to mixing with cooler inlet charge
3) Increased specific heat of intake charge
4) Presence of activated radicals
5) Recycling of unburned hydrocarbons (opportunity for re-burn)

Numerous research works have been carried out by scientists to solve above mentioned issues. Some researchers investigate the effect of EGR on performance and emissions characteristics of dual fuel engines at part loads. Their researches revealed that although use of EGR decreases NO_x emissions but it is not a reliable approach for improving performance and emissions characteristics of dual fuel engines at part loads [10-11-12-13].

This paper touches upon investigating the simultaneous effect of EGR and pre-heating of the inlet air on perfor-mance and emission characteristics of dual fuel engines at part loads. In order to meet future emission standards, EGR must be done over wider range of engine operation, and heavier EGR rate will be needed. Thus, utilizing a spe-cific device to expand EGR area is necessary. In this study, the venturi type EGR system was selected because it is rather effective for expanding the EGR range up to low engine load conditions.

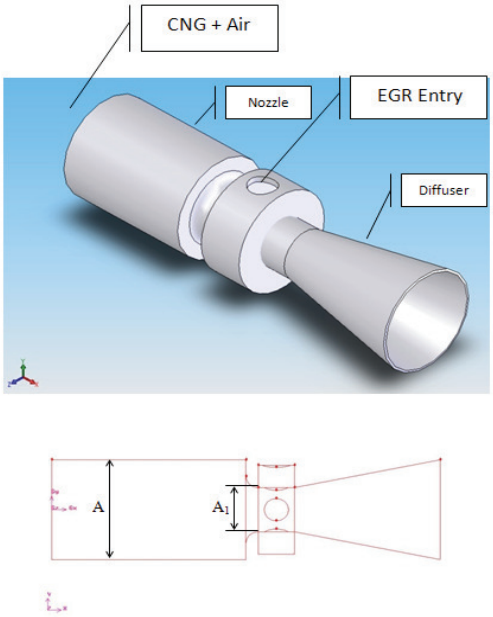

Fig. 1. Schematic of venturi EGR system

2. VENTURI EGR SYSTEM

Due to venturi characteristics there will be a local lowering of the pressure at the venturi throat. Where the pressure is lowered the EGR gases should be lead into the venturi. Therefore, it is theoretically possible for this system to expand the EGR feasible range. Figure 1 shows the configuration of the venturi EGR system. The venturi is located on the intake manifold and consists of three sections: a nozzle, an EGR entry section, and a diffuser. Through the four holes formed on the venturi throat, the EGR gas is drawn into the intake air stream and mixes with the air. The contraction ratio of the venturi is defined as the ratio of the sectional area of the throat to the sectional area of the nozzle (A1/A).

3. CFD ANALYSIS OF VENTURI EGR SYSTEM

3. 1. Computational Domain

The three-dimensional numerical domain constructed using GAMBIT for the current work. Various domains have been modeled in GAMBIT considering the intake manifold diameter.

3. 2. Mesh Generation

To allow the meshing of the domain in a short amount of time, an unstructured mesh consisting of tetrahedral elements was used. Figure 2 shows an overall view of the domain. In keeping with standard

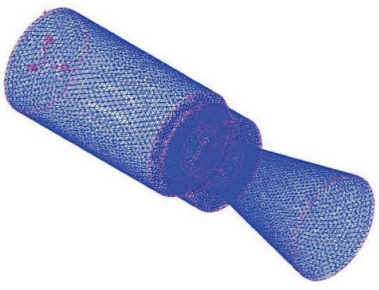

Fig. 2. Overview of the entire mesh

practice care was taken whilst constructing the mesh to ensure that maximum skewness of any of the elements did not exceed 0.7 and that the aspect ratio did not exceed 10:1.

3. 3. Determining "Mesh Independence"

Computational Fluid Dynamics solutions can be sensitive to the level of refinement present in the computational grid. In general, decreasing the size of the grid leads to a loss of accuracy in the solution. The solution is said to be mesh independent when it no longer changes appreciably as the mesh is changed. The initial computational domain is remodeled with a reduced number of mesh elements. The numbers of cells in the venturi regions are summarized in Table 1. For each of two meshes studied here, two CFD cases were run. In the first case, the discretisation schemes for solving the equations for each variable of pressure, density, momentum and turbulent kinetic energy and dissipa-tion rate were calculated using a first-order solution. In the second case a second-order solution was used for the variables.

The mesh independence testing results are summarized in Table 2 for the parameters at the venturi throat. It can be seen from the data that the coarsened mesh leads to a solution agreeing with the original mesh to within 4.2%. This represents an opportunity to significantly reduce the required computational time. A converged solution can be reached within 3 hours on an Intel Core 2 Dou 2.2 GHz CPU and 2 GB of RAM, using the coarse mesh as opposed to the 14 hours required with the original mesh.

Table 1. Total number of mesh elements for grid independence testing

	Total Mesh Count
Initial Mesh	1275335
Coarsened Mesh	244575

Table 2. Sample case mesh independence test results for the venturi

Parameters at Throat	Original Mesh	Coarse Mesh	Difference (%)
Velocity (m/s)	75	71.8	4.2
Temperature (K)	359	352	1.9

3. 4. The Governing Equations

The Navier-Stokes equations are the fundamental partial-differential equations that describe the flow of fluids. For all flows, FLUENT solves conservation equations for mass and momentum.

$$\frac{\partial}{\partial x_j}(\rho\overline{u_i}) = 0 \tag{1}$$

$$\frac{\partial}{\partial t}(\rho\overline{u_j}) + \frac{\partial}{\partial x_i}(\rho\overline{u_i}\overline{u_j}) = \frac{\partial}{\partial x_i}\left(\mu\left[\frac{\partial\overline{u_i}}{\partial x_j} + \frac{\partial\overline{u_j}}{\partial x_i}\right]\right) - \frac{\partial\overline{p}}{\partial x_j} + \rho g_j + \tag{2}$$

For the present work, flows involve compressibility and species mixing, therefore, law of conservation of energy and mass is also solved.

$$\frac{\partial}{\partial t}(\rho y_k) + \frac{\partial}{\partial x_i}(\rho(U_i - U_{\delta i})y_k) = \frac{\partial}{\partial x_i}\left(\Gamma_{yk}\frac{\partial y_k}{\partial x_i}\right) + S_{yk}, k = 1\ldots k_{gas} \tag{3}$$

$$\Gamma_{yk} = \left(\rho D_{k,m} + \frac{\mu_t}{Sc_t}\right), S_{yk} = \dot{r}_k \cdot M_k \cdot V_{Cell} \tag{4}$$

For modeling of the turbulence the standard k-ε model was firstly employed. The standard k-ε model is a two equa-tion eddy viscosity turbulence model [14]. In this model, the eddy viscosity is computed based on the turbulence kinetic energy k, and the turbulence dissipation rate å via:

$$\mu_t = \rho C_\mu \frac{k^2}{\varepsilon} \tag{5}$$

3. 5. Venturi Design Equations

The venturi device as shown in Figure 3 measures the flow rate or velocity of a fluid through a pipe. The equation is based on the Bernoulli equation, conservation of energy, and the continuity equation. The below equations are used for solving flow rate and pressure differential through the venturi [15]. In this study, the objective functions are pres-sure drop and the weight of venturi. They should be minimized optimally to obtain the characteristics of the required venturi.

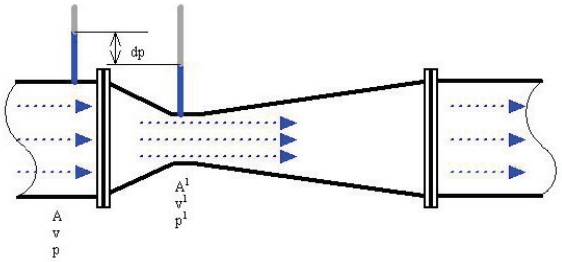

Fig. 3. Schematic of Venturi

$$Q = A_2 \sqrt{\frac{2(p_1 - p_2)}{\rho\left(1 - \left(\frac{A_2}{A_1}\right)^2\right)}} \quad (6)$$

$$(p_1 - p_2) = \frac{\rho}{2} \times \left(1 - \left(\frac{A_2}{A_1}\right)^2\right)\left(\frac{Q}{A_2}\right)^2 \quad (7)$$

3. 6. Boundary Conditions

In the intake part of nozzle and throat entrance, mass-flow inlet type boundaries were used. The NG was modeled as methane. Each case was run with a NG+Air mass-flow set to 0.007244 kg/s which corresponds to the maximum flow rate in the test engine. EGR was considered as combination of H_2O and CO_2 gases. Since the portion of N_2 is less than H_2O and CO_2, EGR was considered as combination of H_2O and CO_2 gases. Temperature of EGR was set to 400 K at the inlet boundary. For the exhaust face of diffuser pressure-outlet boundary was used. For throat holes interior boun-dary was used. Other faces were modeled as wall-boundaries. Initial conditions in the computational domain were set to be quiescent with atmospheric pressure and a temperature of 273 K. The SIMPLE pressure-velocity coupling scheme was used in all cases. The second order discretisation scheme also used in all cases.

3. 7. Selection of Optimum Turbulence Model

To select the optimum turbulence model to implement in the presented study, the two models have been run. The resultant pressure drop across the venturi was compared for the two turbulence models with the value calculated using the standard Equation which calculates the pressure drop. Table 3 gives the validation results. The results show that the realizable k-ε performing slightly better than the standard k-ε model.

Table 3. Pressure drop across the venturi for two turbulence models

Turbulence model	CFD computed Δp (Pa)	Deviation from standard Δp (%)
Standard k-ε	9750	38%
$k-\varepsilon$ Realizable	8250	32%

3. 8. Experimental Results for Venturi EGR System

The combustion process is highly depended on pilot fuel quantity and main fuel's equivalence ratio in dual fuel en-gines. Thus experiments carried out considering engine's different operating load conditions. Each experiment used a different load, ranging from 10% to full load condition. At the load conditions of 10%, 20 %, 40%, 60%, 80% and 100% the pilot fuel is decreased and NG is replaced with it in a way that the engine's torque remained constant at a constant speed and total equivalence ratio did not change. In each case the percentage of EGR rate was measured and compared with original system. Figure 4 shows the advantages of venturi system over the original system in terms of the EGR rate. The original system is a simple pipe which connects the inlet manifold to the EGR system.

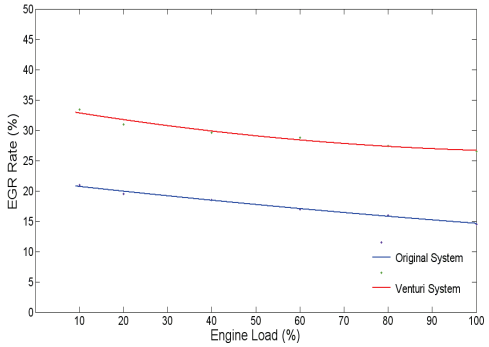

Fig. 4. Advantage of venturi EGR system

4. EFFECT OF VENTURI GEOMETRY

The following section describes the effects of optimizing the shape of each component section by means of FLUENT CFD software. It is a parametric study for finding an optimum venturi. They are selected according to the engine manifold geometric

Table 4. Different cases of venturi component sections for CFD study

Case	Parameter	Shape	Values
Nozzle	Hole diameter	Bell-mouth & cone shape	7.5 mm 10 mm
Diffuser	The length of diffuser to nozzle length $r=L/L_0$	Bell-mouth	0.5 0.75 1
	Contraction ratio $t= A_1/A$	Bell-mouth	0.33 0.44 0.55
Throat	Hole diameter	Bell-mouth	7.5 mm 10 mm

specifications and parameters which are important in designing of a standard venturi. Ten cases were studied in order to find the optimum venturi specifications to expand the EGR range at the part load operation range with minimum pressure loss. The detailed conditions of each case are shown in Table 4.

4. 1. Nozzle

As shown in Figure 5, the shapes of the venturi nozzle, an ordinary cone shape and a bell-mouth shape were chose for this study in order to meet the objectives of compactness and minimum pressure loss. Figure 6 shows the study results. We conducted the simulation for each shape in two cases of hole diameter of 7.5 and 10 millimeters. Regarding the pressure loss, both the shapes showed almost the same characteristics, although the pressure loss of the cone-shaped nozzle was slightly lower than that of the bell-mouth, but the bell-mouth shaped nozzle with shorter overall length was selected because it is much easier to install on the engine intake system.

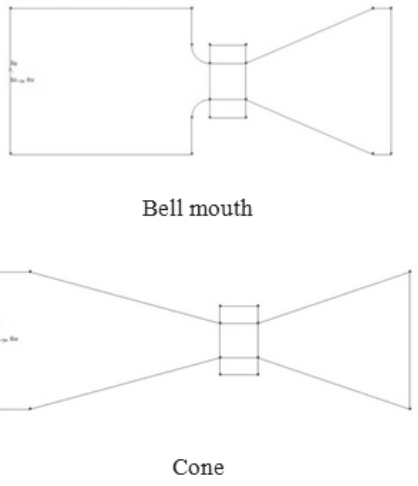

Fig. 5. Shapes of the venturi nozzle

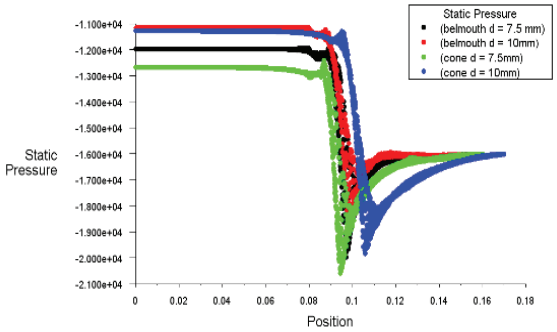

Fig. 6. Effect of nozzle shape on pressure loss along the x direction

4. 2. Diffuser

The shape of the diffuser was also studied to obtain compactness and minimum pressure loss. It is obvious that the pressure loss largely depends upon the expansion angle of the diffuser. Because diffusers can be made more compact by increasing the expansion angle and its length is inversely proportional to the expansion angle, *r* parameter was de-fined as mentioned in Table 4. If the expected increase in the pressure loss can be controlled, the shorter diffuser will significantly reduce the size of venturi. Figure 7 shows the pressure loss for each of the L/L_0 ratios. As a result, in-creasing expansion angle evidently increases pressure loss. Finally, it was determined that the L/L_0 ratio of 0.75 was the most appropriate for the diffuser to be adequately compact while being able to control the pressure loss to a low level.

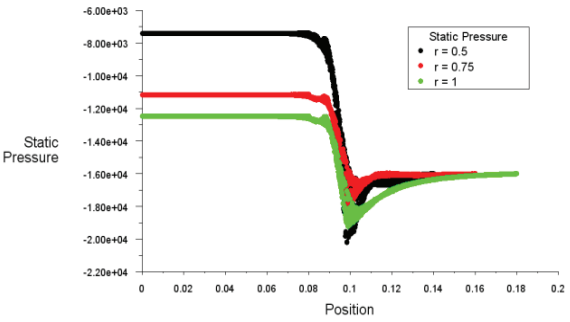

Fig. 7. Effect of diffuser length on pressure loss along the x direction

4. 3. Contraction Ratio

In this part, we considered three different contraction ratios. As it shown in Figure 8, by increasing contraction ratio pressure loss significantly decreases while the size and weight of the venturi increases as well. The simulation results revealed that the optimum contraction ratio was 0.44. It was also confirmed that intake mixture flow did not reach to sonic speed with this contraction ratio.

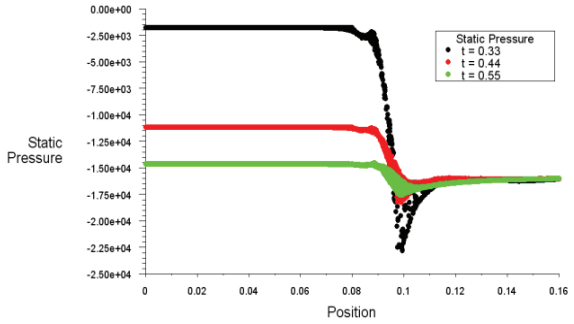

Fig. 8. Effect of contraction ratio on pressure loss along the x direction

4. 4. Effect of Throat Holes Diameter

Finally, the effect of throat holes diameter on the pressure loss was studied. The results are shown in Figure 9. It is obvious that by increasing holes diameters pressure loss slightly increases. Hence, regarding the venturi compactness we chose the 10 mm as an optimum holes diameter.

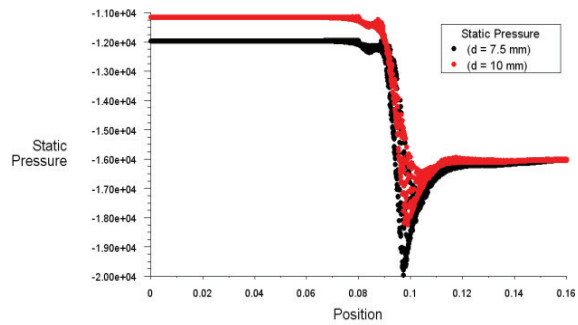

Fig. 9. Effect of throat holes diameter on pressure loss along the x direction

4. 5. Determination of Optimum Venturi Geometry

Based on the results from the simulations and conducted regarding pressure loss and compactness and experiments, it was found that the geometry specifications shown in Table 5 corresponded to the good characteristics of the venturi. The experimental results in section 3.8 showed that the venturi system increased EGR rate to higher levels compared to common system. Pressure, velocity, temperature and species contours are shown in Figure 10-12 for the optimum venturi case.

The optimum venturi manufactured for the tests is shown in Figure 13. Then, it was mounted on the dual fuel en-gine's manifold.

Table 5. Optimum venturi geometry

Contraction Ratio	0.44
Nozzle	Bell-mouth
EGR Entry	d = 10 mm
Diffuser	Expansion Angle $\alpha = 11.85$ Overall Length = 160 mm

5. EXPERIMENTAL SETUP AND PROCEDURE

In the second part of the paper, an experimental investigation was carried out to investigate the effect of exhaust gas recirculation and pre-heating of the inlet air on performance and emission characteristics

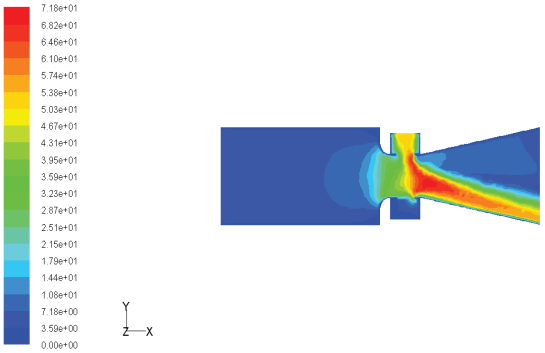

Fig. 10. Velocity distribution contour in the optimum venture

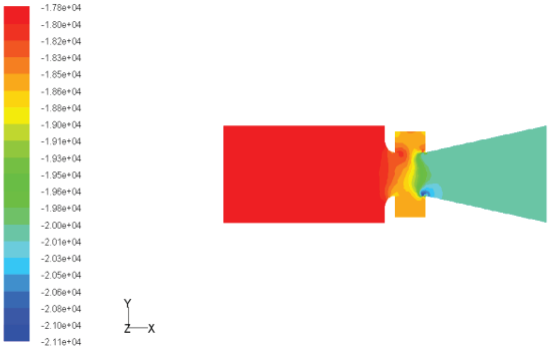

Fig. 11. Pressure distribution contour in the optimum venture

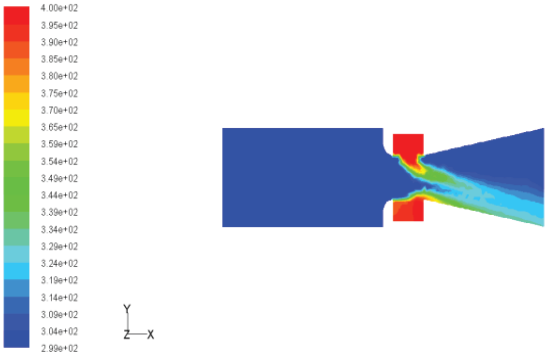

Fig. 12. Temperature distribution contour in the optimum venture

Fig. 13. Schematic of optimum venture

of dual fuel engines at part loads. The engine used for the investigation was a single-cylinder, four-stroke, water cooled, indirect injection (Lister 8-1) dual fuel engine. The technical specifications of the engine are given in Table 6, and the schematic of the

Table 6. General Specifications of Lister (8-1) Dual Fuel engine

Item	Specification
Type	Four Stroke
Number of Cylinders	1
Combustion System	IDI
Bore	114.1 mm
Stroke	139.7 mm
Swept Volume	1.43 Lit
Compression Ratio	17.5:1
Max. power hp/rpm	8/850
Injection Pressure	91.7 kg/cm^2
Injection Timing	20^0 BTDC

experimental setup is shown in Figure 14. The engine is supplied with natural gas obtained from the local distribution network. The gaseous fuel, before entering the engine cylinder, passes through a small tank. The inlet and exhaust air temperatures were measured by K-type thermocouple which is made by Testo Co. The power output of the engine was measured by an electrical dynamometer. The exhaust emissions HC, CO, CO_2 and NOx were measured by AVL 4000 exhaust gas analyzer.

5. 1. EGR System

The EGR system used with the test engine was the type that exhaust gas was recirculated back into the inlet manifold where it mixes with air and natural gas and gets diluted with the intake charge which in turn acts as a diluents and reduces the peak combustion temperature inside the combustion chamber. It included a control valve, pipes and venturi as shown in Fig. 13. To measure the amount of EGR, the parameter EGR ratio was considered. The EGR ratio is defined by [16]

$$\%EGR = \frac{\%CO_2(inlet)}{\%CO_2(outlet)} \times 100 \quad (8)$$

The reported percentages of EGR involved errors up to 5%. For pre-heating the inlet air an electrical heater was used. As shown in Figure 15, it was installed on the intake manifold before the NG mixer.

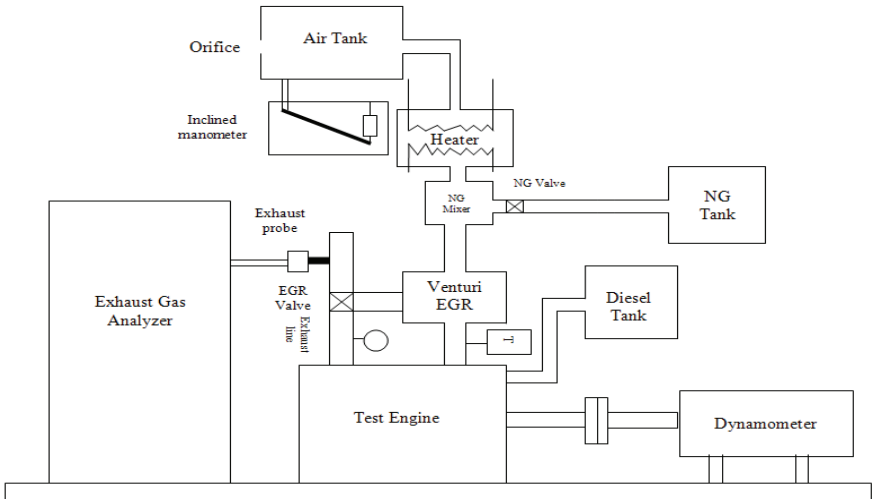

Fig. 14. Schematic diagram of experimental setup

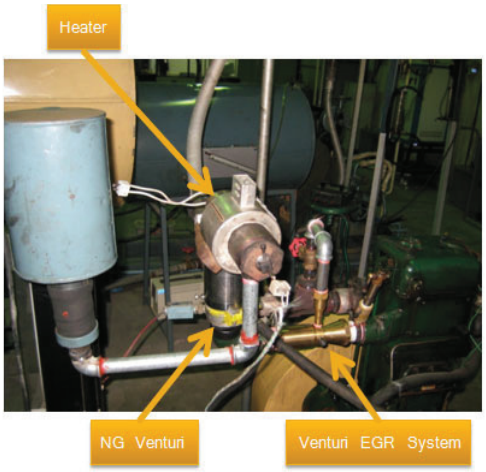

Fig. 15. Venturi EGR system on the in the intake manifold

Table 7. Average uncertainties of some measured and calculated parameters

S. no	Parameters	Uncertainty (%)
1	Speed	1.1
2	Temperature	0.8
3	Mass flow rate of air	1.7
4	Mass flow rate of diesel	3.5
5	Mass flow rate of natural gas	4.1
6	Oxides of nitrogen	2.2
7	Unburned hydrocarbons	2.9
8	Carbon monoxide	3.3
9	EGR rate	5

5. 2. Test Conditions Examined

The engine was started with diesel fuel; later the diesel was reduced and natural gas was supplied to the intake mani-fold. Under dual fuel operation, an effort has been made to keep the pilot amount of diesel fuel constant, while the power output of the engine is adjusted through the amount of gaseous fuel. Natural gas flow increased until the en-gine reached the rated speed of 730 rpm.

6. ESTIMATION OF UNCERTAINTY

Any experimental measurement possesses a certain amount of uncertainty. The uncertainty in any measurement may be due to either fixed or random errors. As the fixed errors are repeatable in nature they can be easily accounted for to get the true value of measurement. However, random errors have to be estimated only analytically. In this paper, the main focus is on quantification of random sampling error, which is the statistical random fluctuation in any statistic estimated from a finite random sample of data. Uncertainty due to random sampling error may often be a large or even dominant source of uncertainty for small data sets that are highly skewed. In this study, Weibull distribution was considered for representing variability in data sets. Bootstrap simulation is used to quantify uncertainty based upon random sampling error [17]. The details of the estimated average uncertainty of some typical operating conditions are given in Table 7. It can be seen that the uncertainty ranges from 0.8% to 5%.

7. RESULTS AND DISCUSSION

In the present work, performance and emission characteristics of a dual fuel engine at part loads were studied for two different cases. For the purpose of comparison, first, the dual fuel engine was operated at part loads using differ-ent EGR flow rates to study performance and emission characteristics of Lister 8-1 dual fuel engine. In second case, combination effect of EGR and preheating the inlet air on performance and emission characteristics of the dual fuel engine at part loads were studied.

7. 1. Effect of EGR on Performance and Emission Characteristics of the Dual Fuel Engine at Part Loads

7. 1. 1. Brake Thermal Efficiency

Figure 16 shows the variations of brake thermal efficiency for different EGR rates at part loads. The brake thermal efficiency increases at low EGR ratios. The increase in thermal efficiency for low EGR ratios, at part loads is due to the recirculation of active radicals from EGR and achievement of richer fuel air mixture than the baseline case that makes the combustion process to be enhanced, so resulting in an improvement in brake thermal efficiency. However, increasing EGR flow rates to high levels resulted in decrease in brake thermal efficiency. The reduction in thermal efficiency is due to the high EGR ratios that results in deficiency in oxygen concentration in combustion process at part loads and larger replacement of air by EGR. The higher specific heat capacity of both CO_2 and H_2O and high flow rates of EGR reduces the average combustion temperature in the combustion chamber resulting in the brake thermal efficiency to reduce at high EGR flow rates.

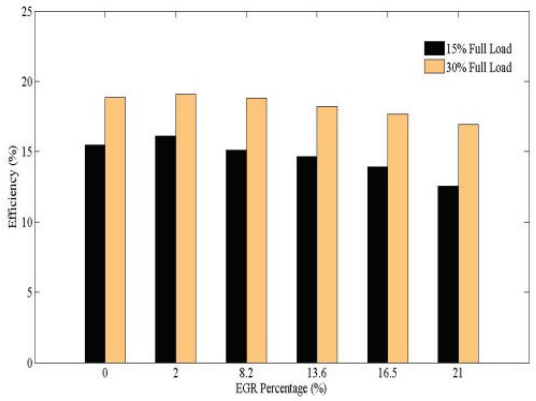

Fig. 16. Variation of brake thermal efficiency for different EGR flow rates at part loads

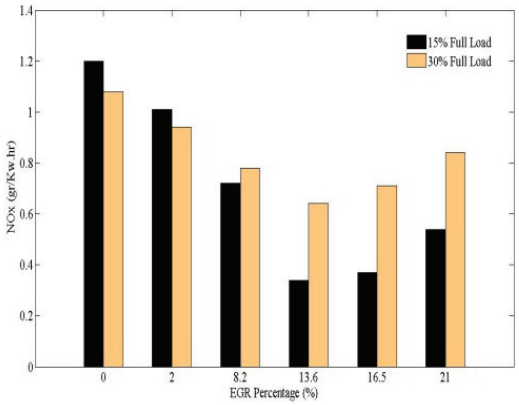

Fig. 17. Variation of oxides of nitrogen for different EGR flow rates at part loads

7. 1. 2. Oxides of Nitrogen

Figure 17 depicts the variation of NO_x emissions at part loads for different EGR flow percentages. Generally, the NO_x emissions tend to decrease significantly with increase in EGR ratio for all load conditions due to the rise in total heat capacity of combustion chamber charge by EGR, which lowers the peak combustion temperatures. The NO_x emission reduces with increase in EGR flow percentage, this is due to the fact that presence of inert gases such as CO_2 and H_2O in the combustion chamber reduces the peak combustion temperature, and also it replaces the oxygen in the combus-tion chamber. As a result of reduction in both parameters the NO_x decreases with EGR. However, at high EGR flow rates, NO_x emissions tend to increase. It can be due the negative effects of EGR that may overcome to its positive effects.

7. 1. 3. Unburned Hydrocarbons

The variation of UHC emissions at part loads for different EGR flow rates is shown in Figure 18. As seen from this figure, THC emissions at low loads are relatively high. This is due to the poor combustion of the resulting very lean (overall) natural gas mixtures

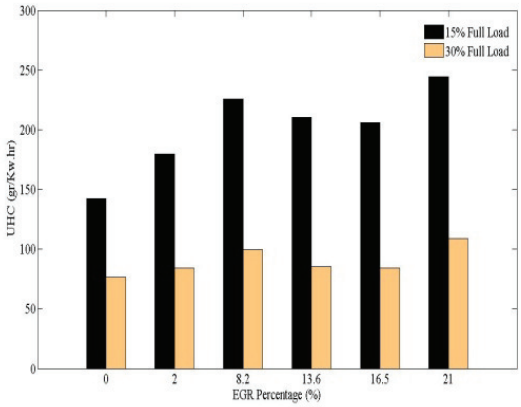

Fig. 18. Variation of unburned hydrocarbons for different EGR flow rates at part loads

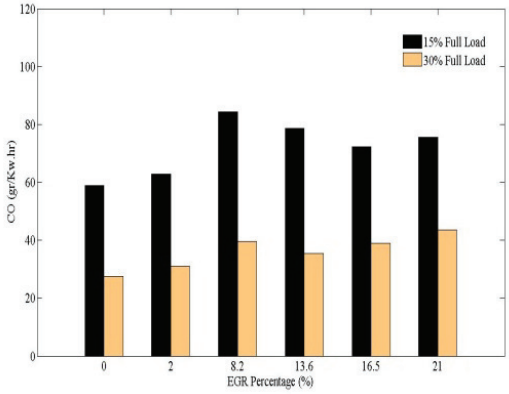

Fig. 19. Variation of carbon monoxide for different EGR flow rates at part loads

causing high levels of unburned or partially-burned fuel in the exhaust [10]. The HC variation follows a close trend with increase in EGR ratio resulting in increase in HC emission. The increase in HC emissions is due to the effect of flame quenching at part load, also reduction in oxygen concentration in the inlet charge by the EGR introduced into the cylinder makes the HC emissions to increase. However, increasing EGR flow rate to high levels resulted in decrease in HC emissions. One reason for this is that a portion of the unburned gases in the exhaust from the previous cycle is recirculated and burned in the succeeding cycle. Furthermore, the presence of radicals can help to initiate the combustion process, especially with increase of intake charge temperature due to mix-ing with exhaust gases. On the other hand, the diluents try to stop the reactions, but the combined effects of radicals and intake temperature are dominant [18].

7. 1. 4. Carbon Monoxide

The variation of carbon monoxide with load and with varied flow rate of EGR percentage is shown in Figure 19. With increase in EGR percentage at part loads CO emissions tend to increase slightly. The increase in CO concentration is due to the partial replacement of oxygen in inlet air by inert gas, which results in deficiency in oxygen concentration, hence increasing the CO concentration. However, increasing EGR flow rates to high levels resulted in decrease in amount of CO emissions. The reduction in CO at part loads due to the high EGR percentages is that it creates a hotter environment, which makes the combustion to improve.

7. 2. Effect of Pre-Heating Inlet Air and EGR on Performance and Emission Characteristics of the Dual fuel Engine at Part Loads

In order to study the effects of EGR combined with intake preheating on performance and exhaust gas emissions of a dual fuel engine at part loads, according to Table 8 the experiments conducted at a constant engine speed of 730 rpm.

Table 8. Engine tests conditions for intake heating combined with EGR (engine speed: 730 rpm, load: 1/5 full load, NG fraction: 75%)

CASE	EGR ratio (%)	Intake Mixture Temperature (K)	EGR ratio (%)	Intake Mixture Temperature (K)
Constant EGR Percentage & Variations of Intake Mixture Temperature	13.5	373	18.5	373
		383		383
		403		420
		425		440
Constant Intake Mixture Temperature & Variations of EGR Percentage	13.5	355	13.6	430
	17.5		16.5	
	19		19.5	

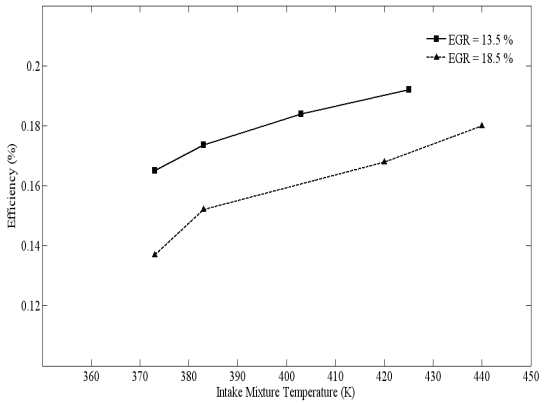

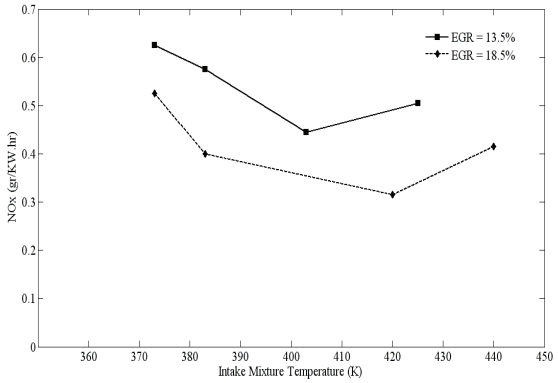

Fig. 20. Variation of brake thermal efficiency with intake mixture temperature at constant EGR flow rates (load: 1/5, NG fraction: 75%)

7. 2. 1. Constant EGR Percentage & Variations of Intake Mixture Temperature

7. 2. 1. 1. Brake Thermal Efficiency

Figure 20 shows the effects of preheating inlet air combined with EGR at 75% natural gas fraction and 15% of full load. It is clear that remarkable improvements in thermal efficiency obtained in this case. This is due to the in-creased intake temperature. The increase of intake temperatures will accelerate the reaction rates of the mixture, widen its flammability limits and sustains flame propagation within relatively leaner mixtures. Thus, increasing the intake temperature will produce higher charge temperatures which lead to propagating the flame successfully through the gaseous fuel air mixture [18].

7. 2. 1. 2. Oxides of Nitrogen

Figure 21 portrays the variation of oxides of nitrogen with intake mixture temperature at constant EGR flow rates. It can be observed that the NO_x emissions decrease as the EGR ratio increases. On the other hand, The NO_x emissions reduce with increase in intake mixture temperature; so, the optimum intake temperature in which the minimum NO_x can be achieved is 410 K approximately. This can be explained by the fact that the inert gas included in the recircu-lated exhaust gas decreased the combustion temperature in spite of intake pre-heating. Thus, pre-heating of inlet air combined with EGR has two favorable effects on combustion. One is the increased cylinder temperature, which leads to improved combustion of natural gas in the premixed charge. This results in improvements in both brake thermal efficiency and UHC emission. The other favorable effect is decreased level of NO_x due to the inert gas [19]. However, NO_x emissions tend to increase at high intake mixture temperatures. The presence of radicals can help to initiate the combustion process, especially with increase of intake mixture temperature due to mixing with exhaust gases. Although the diluents try to stop the reactions, but the combined effects of radicals and intake temperature are dominant. Hence, the NO_x increases with increasing intake mixture temperature.

7. 2. 1. 3. Unburned Hydrocarbons

The variation of unburned hydrocarbons with intake mixture temperature at constant EGR flow rates is depicted in Figure 22. The UHC values are lesser for high EGR ratios. It can be seen that increasing the intake mixture tempera-ture had a beneficial effect in reducing unburned hydrocarbon emissions. One reason for this is that a portion of the unburned gases in the exhaust from the previous cycle is recirculated and burned in the succeeding cycle. On the other hand, increasing intake mixture temperature decreases ignition delay and results in improvements in combus-tion process. At low loads, the flame cannot propagate successfully, which leads to increase in the UHC emissions.

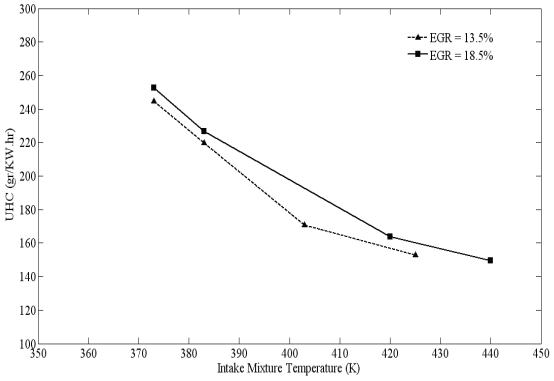

Fig. 22. Variation of unburned hydrocarbon with intake mixture temperature at constant EGR flow rates (load: 1/5, NG fraction: 75%)

7. 2. 1. 4. Carbon Monoxide

The variation of carbon monoxide with intake mixture temperature at constant EGR flow rates is shown in Figure 23. The CO variation follows a close trend with increase in intake mixture temperature resulting in decrease in CO emission.

The increase of intake mixture temperatures will accelerate the reaction rates of mixture, widen its flammability limits and sustain flame propagation within relatively leaner mixtures. Thus, increasing the intake temperatures lead to propagating the flame successfully through the gaseous fuel air mixture. This can possibly reduce CO in the ex-haust. Also, the high EGR percentages create a hotter environment, which makes the combustion to improve. The results obtained show a good agreement according to Kusaka et al. work. They showed that EGR combined with intake pre-heating can reduce NOx and THC with improved thermal efficiency [19].

7. 2. 2. Constant Intake Mixture Temperature & Variations of EGR Percentage

7. 2. 2. 1. Brake Thermal Efficiency

Figure 24 shows the Variation of brake thermal efficiency with different EGR flow rates at constant intake mixture temperatures. The brake thermal efficiency decreases slightly with increasing EGR flow rate at both constant intake temperatures. The reduction in thermal efficiency is due to the EGR that results in deficiency in oxygen concentra-tion in combustion process at part loads and larger replacement of air by EGR. The higher specific heat capacity of both CO_2 and H_2O and high flow rates of EGR reduces the average combustion temperature in the combustion chamber resulting in the brake thermal efficiency to reduce.

7. 2. 2. 2. Oxides of Nitrogen

Figure 25 depicts Variation of oxides of nitrogen with different EGR flow rates at constant intake mixture tempera-tures. The NO_x emissions reduce with increase in EGR flow percentage at constant intake mixture temperatures. The combustion temperature and local oxygen concentration are dominant parameters for NO_x formation. The presence of inert gases in the combustion chamber reduces the

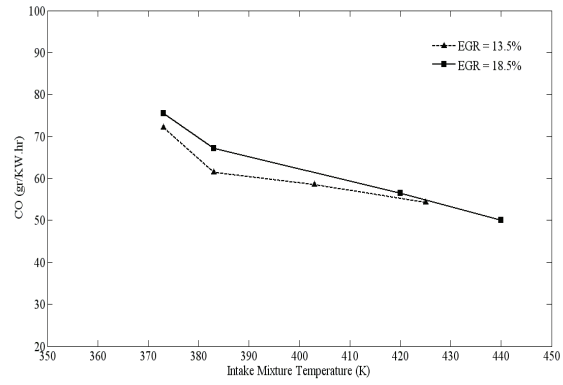

Fig. 23. Variation of carbon monoxide with intake mixture temperature at constant EGR flow rates (load: 1/5, NG fraction: 75%)

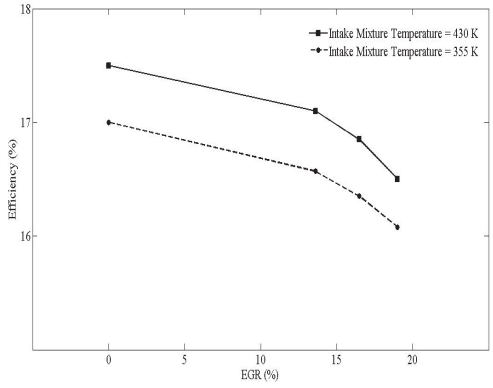

Fig. 24. Variation of brake thermal efficiency with different EGR flow rates at constant intake mixture temperatures (load: 1/5, NG fraction: 75%)

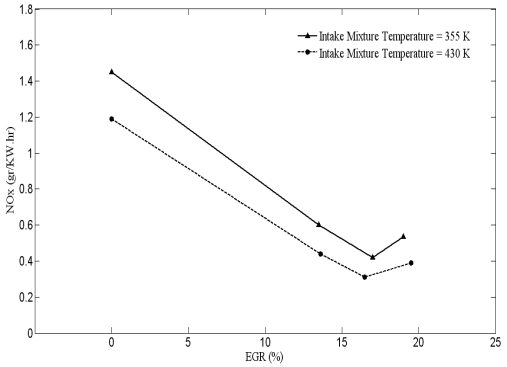

Fig. 25. Variation of oxides of nitrogen with different EGR flow rates at constant intake mixture temperatures (load: 1/5, NG fraction: 75%)

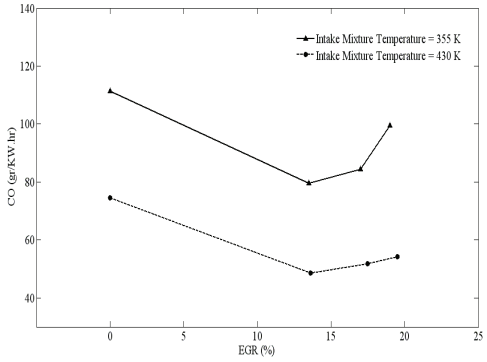

Fig. 27. Variation of carbon monoxide with different EGR flow rates at constant intake mixture temperatures (load: 1/5, NG fraction: 75%)

peak combustion temperature, and also it replaces the oxygen in the combustion chamber. As a result of reduction in both parameters the NOx decreases with EGR. However, at high EGR flow rates, NO_x emissions tend to increase. It can be due the negative effects of EGR that may overcome to its positive effects.

7. 2. 2. 3. Unburned Hydrocarbons

The variation of unburned hydrocarbon with different EGR flow rates at constant intake mixture temperatures is shown in Figure 26. As seen from this figure, UHC emissions are lower at high intake mixture temperatures, whereas increasing EGR ratio caused a drop in unburned hydrocarbon emissions. One reason for this is that the presence of radicals in the recirculated exhaust gases can help to initiate the combustion process, especially with increase of intake charge temperature due to mixing with exhaust gases.

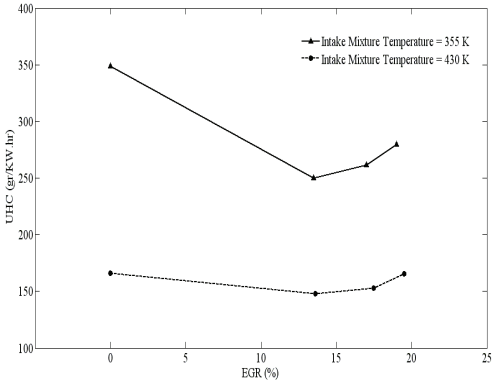

Fig. 26. Variation of unburned hydrocarbon with different EGR flow rates at constant intake mixture temperatures (load: 1/5, NG fraction: 75%)

7. 2. 2. 4. Carbon Monoxide

The variation of carbon monoxide with different EGR flow rates at constant intake mixture temperatures is de-picted in Figure 27. It is obvious that CO emission is lower at high intake mixture temperatures, while increasing EGR flow rate resulted in a decrease in carbon monoxide emissions. This is due to the fact that the EGR combined with high intake mixture temperatures create a hotter environment, which accelerate the reaction rates of mixture and as a result, make the combustion to improve. However, CO emission tends to increase at high EGR percentages. This may mainly due to the partial replacement of oxygen in inlet air by inert gas, which results in deficiency in oxygen concentration.

8. CONCLUSIONS

A venturi EGR system has been studied numerically to find an optimum device for introducing high amount of EGR to the dual fuel engine manifold. An experimental investigation has been also conducted to examine Effect of ex-haust gas recirculation and pre-heating of the inlet air on performance and emission characteristics of the dual fuel engines at part loads. Based on the results the following conclusions were obtained:

1. The CFD analysis carried out revealed that the

venturi should be optimized to increase the EGR rate at the part load operation range with minimum pressure loss.

2. The experimental results show a slight trend of increase in EGR rate with decrease in engine load. There is lower amount of air and NG at engine's part load operation, since venturi system involves pressure losses at the nozzle and diffuser sections, it would be able to introduce higher amount of EGR to the intake manifold.
3. The brake thermal efficiency, CO and UHC emissions increased, but, NO_x decreased at low EGR flow rates. However, high EGR percentages resulted in a decrease in thermal efficiency, CO and UHC emissions, although NOx increased in this case.
4. Constant EGR percentages combined with variation of intake mixture temperature can favorably increase brake thermal efficiency and decrease CO, UHC and NO_x emissions.
5. From these above points of view, EGR combined with pre-heating of inlet air reduces NO_x, UHC and CO emissions without deteriorating engine thermal efficiency.

ACKNOWLEDGEMENT

This work is supported by the fund of Tabriz Oil Refinery Company which is highly acknowledged.

REFERENCES

[1] O. Bahr, G.A. Karim, B. Liu, An examination of the flame spread limits in a dual fuel engine, Int. J. Appl. Thermal Eng. 19 (1999) 1071–1080.

[2] V. Pirouzpanah, B.O. Kashani, Prediction of major pollutants emission in direct-injection dual-fuel diesel and natural gas engines, SAE Paper 990841 (1999).

[3] A. Henham, MK. Makkar, Combustion of simulated biogas in a dual-fuel diesel engine. Energy Conversion and Management 1998;39(16–18):2001–9.

[4] R. Scarcelli, Lean-burn operation for natural gas/air mixtures: The dual fuel engines", PhD thesis in mechanical engineering, faculty of mechanical engineering, Roma, Italy, 2007.

[5] T. Sato, T. Saito, Y. Daisho, Combustion and exhaust emission control in a dual-fuelled engine, SAE Paper No.9305346, 1993.

[6] CS. Weavar, SH. Turner, Dual fuel natural gas/diesel engines: Technology, performance and emissions, SAE Paper No. 940548, 1994.

[7] B.B Sahoo, N. Sahoo,U.K Saha, Effect of engine parameters and type of gaseous fuel on the performance of dual-fuel gas diesel engines – A critical review", Renewable and Sustainable Energy Reviews, 2008.

[8] H Yokomura, S. Kohketsu, K. Mori, EGR system in a turbocharged and intercooled heavy-duty diesel engine; Expansion of EGR area with venturi system, technical review, Mitsubishi Motors Corporation, 2003.

[9] K.K Srinvasan , S.R.Krishnan , Y.Qi , C.Midkiff , H.Yang , Analysis of diesel pilot-ignited natural gas low-temperature com-bustion with hot exhaust gas recirculation". Combustion Sci. and Tech, 179: 1737-1776, 2007.

[10] Y. Daisho, T. Yaeo, T. Koseki, T. Saito, R. Kiahara. Combustion and exhaust emissions in a direct-injection diesel engine dual-fueled with natural gas, SAE Paper, 950465, 1995.

[11] G.H. Abd-Alla, Using exhaust gas recirculation in internal combustion engines, Energy Conversion and Management 43, 1027-1042, 2002.

[12] Y.E.M. Selim, Effect of exhaust gas recirculation on some combustion characteristics of dual fuel engine, Energy Conversion and Management 44,707-721, 2003.

[13] V. Pirouzpanah, R. Khoshbakhti Saray, Reduction of emission in an automotive direct injection diesel engine dual-fueled with natural gas by using variable exhaust gas recirculation, Proc. Instn Mech. Engrs, Part D: Automobile Engineering, Vol-217:719-725, 2003.

[14] B.E Launder, D.B Spalding. Lectures in mathematical models of turbulence. Academic press, London, 1972.

[15] B.R. Munson, D. F. Young, and T. H. Okishi. Fundamentals of Fluid Mechanics. John Wiley and Sons, Inc. 2nd edition. 1994.

[16] V. Pirouzpanah, R. Khoshbakhti Saray, A. Sohrabi, and A. Niaei, Comparison of thermal and radical effects of EGR gases on combustion process in dual fuel engines at part loads,

Journal of Energy Conversion and Management, Vol. 48:1909-1918. 2007.

[17] S. Li, Development and demonstration of a methodology for characterizing and managing uncertainty and variability in emission inventories. PhD Thesis , North Carolina State University, 2002.

[18] G.H. Abd-Alla, H.A. Soliman, O.A. Badr, M.F. Abd-Rabbo, Effect of diluents admissions and intake air temperature in exhaust gas recirculation on the emissions of an indirect injection dual fuel engine", Energy Conversion and Management 42, 1033-1045, 2001.

[19] J. Kusaka, Y. Daisho, R. Kiahara, T. Saito and SH. Nakayama, Combustion and exhaust gas emissions characteristics of a diesel engine dual-fueled with natural gas. The fourth international symposium COMODIA, 555-660, 1998.

Nomenclature

$D_{k,m}$	Diffusion Coefficient
V_{cell}	Volume of the computational cell
EGR	Exhaust Gas Recirculation
y_k	Mass fraction of a chemical species
M_k	Molecular Weight
η_{th}	Thermal Efficiency
$\dot{r}_k$	Reaction rate of species
Δp	Pressure drop (Pa)
Sc_t	Turbulent Schimdt number
A	Area (m^2)